(Received 24 May 2024, Accepted 29 July 2024, Scheduled 14 August 2024)

A Miniaturized Tag Antenna Based on Meandered Line Technique for UHF Radio Frequency Identification Applications

El Mustapha Louragli[1], Younes El Hachimi[1], Sudipta Das[2,*], Tanvir Islam[3], Boddapati Taraka Phani Madhav[4], and Abdelmajid Farchi[1]

[1] *Laboratory of Engineering, Industrial Management and Innovation (IMII), Faculty of Sciences and Technologies University Hassan 1st, Settat, Morocco*
[2] *Department of Electronics and Communication Engineering, IMPS College of Engineering and Technology Malda-732103, West Bengal, India*
[3] *Department of Electrical and Computer Engineering, University of Houston, Houston, TX 77204, USA*
[4] *Antennas and Liquid Crystal Research Center, Department of ECE, Koneru Lakshmaiah Education Foundation, AP, India*

ABSTRACT: The current paper describes a compact, long-reading-range tag antenna for radio frequency identification (RFID) applications in the ultra-high frequency (UHF) band, operating at 915 MHz. The antenna's miniaturized design is achieved through the utilization of the meandering line technique. A T-matching structure matches the chip impedance to that of the antenna. Polytetrafluoroethylene, or PTFE, is used as the substrate for fabrication. The UHF tag's physical dimensions are $44.4 \times 14.4 \times 0.8\,\text{mm}^3$. This antenna was first designed, simulated, and then optimized by the software Computer Simulation Technology-Microwave Studio (CST-MWS) before being fabricated. The measured reflection coefficient at 915.5 MHz is approximately -24 dB, exhibiting a bandwidth of 7,9 MHz (911.5 MHz–919.4 MHz). The proposed tag is shown to have a gain of 1.56 dB and radiation efficiency of 90% at the resonant frequency of 915 MHz. Its long reading range at 915 MHz is roughly 18.41 m, for an EIRP of 4 W. The measured results closely align with the simulated ones.

1. INTRODUCTION

Radiofrequency identification constitutes a technological approach that utilizes electromagnetic fields to recognize and track objects automatically. It differs from other automatic identification technologies like barcode systems and optical character recognition offering the possibility of tracking objects at several distances without the need for a direct line of sight [1]. It also has the capability to read a large number of objects simultaneously including those in motion. Due to its numerous advantages, RFID has garnered significant attention in various sectors such as healthcare, military, electronic payment systems, libraries, access control, and agriculture [2, 3]. RFID technology consists mainly of three components: tags, readers, and intermediate data processing and management systems [4]. The reader comprises a transceiver and scanning antennas that transmit and receive the ta's signals. The RFID tags are typically subdivided into passive and active categories. The latter are supplied by an onboard battery, while passive ones are supplied using electromagnetic waves emitted by the reader [4, 5]. Unlike active RFID tags, passive tags have no on-board power supply, making them smaller and therefore easier to transport for a variety of applications. Once activated, the tag automatically sends digital information to the reader, which translates this signal into a unique item of identification data. Thus, the tag is a vital component of RFID systems, as its performance directly impacts the overall system performance [6]. It is composed of an antenna and a microchip that stores the data relating to the tag. The chip's impedance is complex which necessitates designing an antenna that matches the chip's impedance.

RFID technology can operate at several frequency ranges [7]: LF (125–134 kHz), HF (13.56 MHz), UHF (840–960 MHz), and microwave (2.45 and 5.8 GHz). Each band has its own characteristics such as the data transfer rates and the maximum reading distance for RFID tag detection. The range of frequencies available for UHF RFID differs from region to region, i.e., 865–868 MHz in Europe and Africa, 902–928 MHz in America/Canada, 908.5–914 MHz in Korea, and 950–956 MHz in Japan [6]. Contrary to LF and HF bands, UHF attracts more interest, owing to fast data transfer speed, long read ranges, and capabilities for reading many tags [8]. In recent years, there have been high-end demands from consumers for light, thin, and small tags, with a low-cost and easy manufacturing process that can be suitable to be implemented on small items [9]. This situation has prompted researchers to develop innovative passive UHF RFID tag antennas with miniaturized size, simple configuration, and an easy and fast fabrication process to cater to the consumer's needs. The tag antenna needs to exhibit a highly radiating efficacy to acquire a high read range. Additionally, the reading range can also be enhanced by appropriately matching the chip and antenna impedance [10]. Therefore, antenna design for passive UHF RFID tags poses challenges, including achieving proper impedance matching and miniaturization simultaneously while maintaining a less complex antenna structure. Numerous methods are employed to attain miniaturized designs for RFID tags: high-permittivity ceramic sub-

* Corresponding author: Sudipta Das (sudipta.das1985@gmail.com).

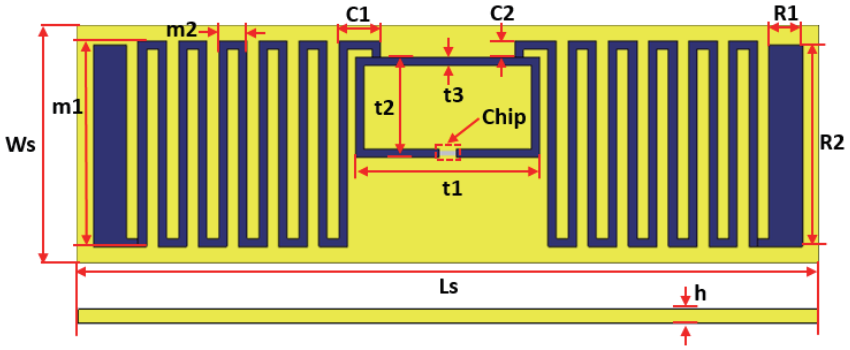

FIGURE 1. Geometry of the proposed antenna.

strates [11], shorting pins [12], and meander lines [13, 14]. The utilization of high-permittivity ceramic substrates and shorting pins requires a complex and costly fabrication process. To resolve this problem, the meander line technique is a renowned approach to reducing RFID tag dimensions. By elongating the current path, it effectively extends the electrical length, resulting in reduced antenna size without increasing the cost and complexity of fabrication. A perfect coupling impedance must be achieved between the tag and the chip to increase the RFID tag's efficiency. Numerous techniques have been proposed for this reason: T-match network [15], inductively coupled loop [16], and the inclusion of nested slots [17]. T-match network has been a favorite method used by the researchers while modeling tag's antenna. Indeed, the chip's impedance can be adapted to that of the antenna, while preserving the antenna's overall size.

Within this paper, a miniatured antenna for UHF RFID tags is conceived to offer good matching, a long reading range, and high radiation efficiency. The antenna operates in the UHF band with a 7.9 MHz bandwidth extending from 911.5 MHz to 919.4 MHz. The suggested design comprises a T-matching structure, meander lines, and a radiator, implemented on an inexpensive polytetrafluoroethylene (PTFE) substrate. Polytetrafluoroethylene (PTFE) was chosen as the substrate material to obtain a better gain for the designed RFID tag. Simulation results show good agreement with measurements. This article's remaining sections are divided in the following manner. Section 2 describes the suggested antenna design, followed by a parametric study (Section 3). A discussion of the results is provided in Section 4, and lastly, a concluding section in Section 6.

2. ANTENNA DESIGN

The suggested miniatured antenna configuration is depicted in Fig. 1. To construct this antenna, a 0.035 mm layer of copper is engraved on a single-layer polytetrafluoroethylene (PTFE) plate ($\varepsilon r = 2.55$, $\tan\delta = 0.0015$) of 0.8 mm thick. The entire tag antenna measures $44.4 \times 14.4 \times 0.8\,\text{mm}^3$. It consists of a T-match, meander lines, and radiators, making it simple. In RFID applications, the input impedance of the RFID chip is not equal to 50 Ω. The chip's impedance is complex. It is necessary that the input impedance of the antenna must be equal to the conjugate impedance of the chip to obtain a good adaptation allowing maximum power transfer and increase the RFID tag's efficiency. For this purpose, the suggested T-match structure has been used. By modifying the dimensions of the T-match structure, the value of the antenna impedance can be changed, thus ensuring good impedance matching between the antenna and the chip. In summary, the T-match is utilized to ensure conjugate matching with the chip, thus ensuring a good adaptation. The meander line reduces the antenna's physical size. The parameters that have been optimized are detailed in Table 1. The microchip used is the Alien Higgs-4 [18], with a threshold power sensitivity value of −20.5 dBm. Fig. 2 shows the internal RC circuit of this chip, where $R = 1.8\,\text{K}\Omega$ and $C = 0.89\,\text{pF}$. The chip impedance is frequency-dependent, with a complex impedance of $Zc = 18.43 - j181.2\Omega$ at 915 MHz, calculated using the following formula:

TABLE 1. Antenna dimension.

Paramete	Ls	Ws	h	t1	t2	t3
In mm	44.4	14.4	0.8	11	6	0.5
Paramete	R1	R2	C1	C2	m1	m2
In mm	2	12.15	2.5	1	12.4	1.7

$$Z_C = \frac{R}{1+4\pi^2 f^2 R^2 C^2} - j\frac{2\pi f R^2 C}{1+4\pi^2 f^2 R^2 C^2} \quad (1)$$

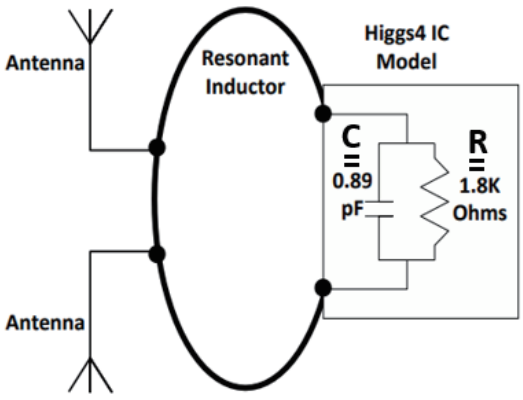

FIGURE 2. The internal RC circuit schematic of Alien Higgs-4 microchip.

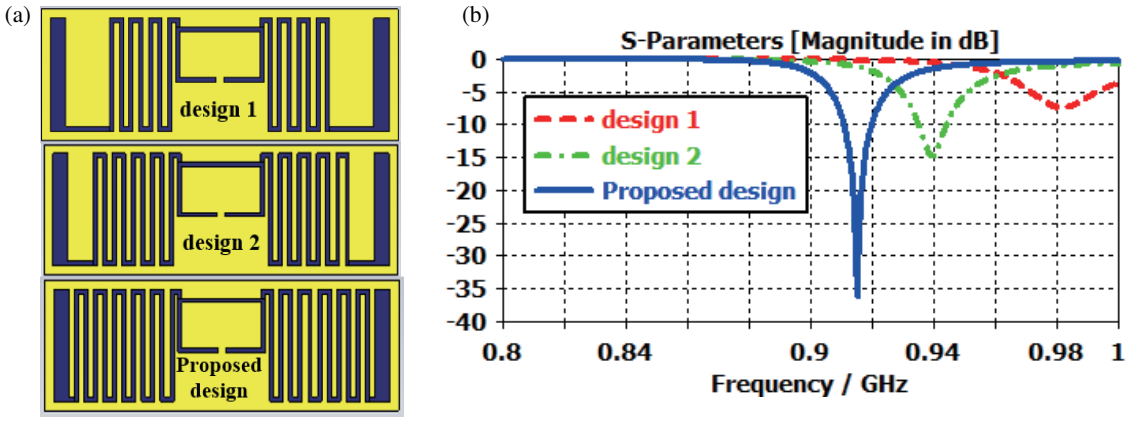

FIGURE 3. (a) Suggested structure design according to the number of meander lines. (b) Simulated reflection coefficient for each design.

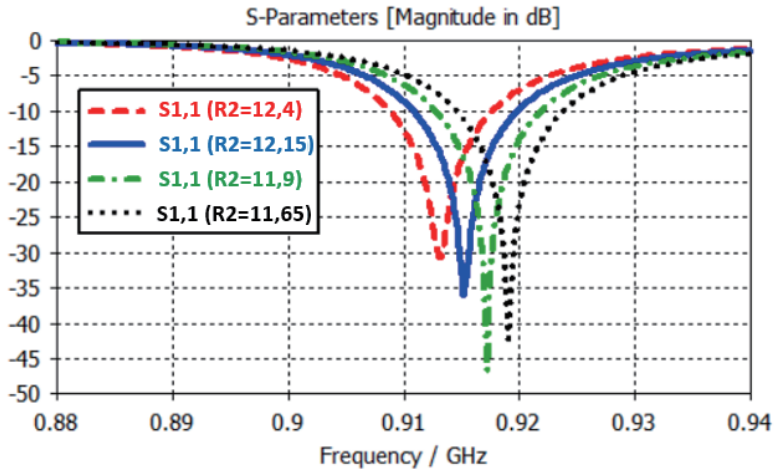

FIGURE 4. Simulated reflection coefficient of the suggested structure vs various radiator lengths.

As RFID chips are capacitive by nature, tag antennas have to be designed with an inductive impedance to ensure maximum power transfer. Consequently, the antenna input impedance, Za, is required to be the chip's conjugate impedance. To lodge the chip, a tiny 1 mm gap is located in the center of the T-match to lodge the chip. The antenna design was carried out via CST-MWS. Initially, a 50 Ω port was applied to determine the suggested antenna impedance. Subsequently, an additional lumped port was added to normalize the port to account for the chip's complex impedance at feeding terminals, which would allow the plotting of the intended tag's reflection coefficient.

3. PARAMETRIC STUDY

The antenna's performance is influenced by its geometric parameters. Through a series of simulations using CST-MW, parametric research is conducted aiming at enhancing the suggested structure's performance. This study aims to demonstrate the impact of altering the number of meander lines, the length of the radiator, and the T-matching structure dimensions on the antenna's performance. Each physical parameter of the design is varied independently while retaining the others at constant dimensions

3.1. Impact of Meander Lines Number Variation on the Reflection Coefficient

The first simulation study concerns how changing the meander line number affects the resonance frequency. Fig. 3(a) shows the modifications performed to our proposed antenna by acting on the number of meander lines while keeping the overall dimensions of the antenna unchanged. Fig. 3(b) illustrates the reflection coefficient obtained for each design. Resonance frequency is obviously shifted to lower frequencies, and impedance matching improves as the meander's line number rises. It means that increasing the length of the meander lines by elongating the current path will extend the tag antenna's electrical length. The meandering line technique has enabled the reduction of the antenna's size, operating within RFID UHF band.

3.2. Impact of Varying Radiator Length ``R2'' on the Reflection Coefficient

The study is carried out on the radiator length "R2". Fig. 4 demonstrates the changing effect of radiator length "R2" on the reflection coefficient of the Tag while retaining the other parameters constant. The figure reveals that, by altering the R2

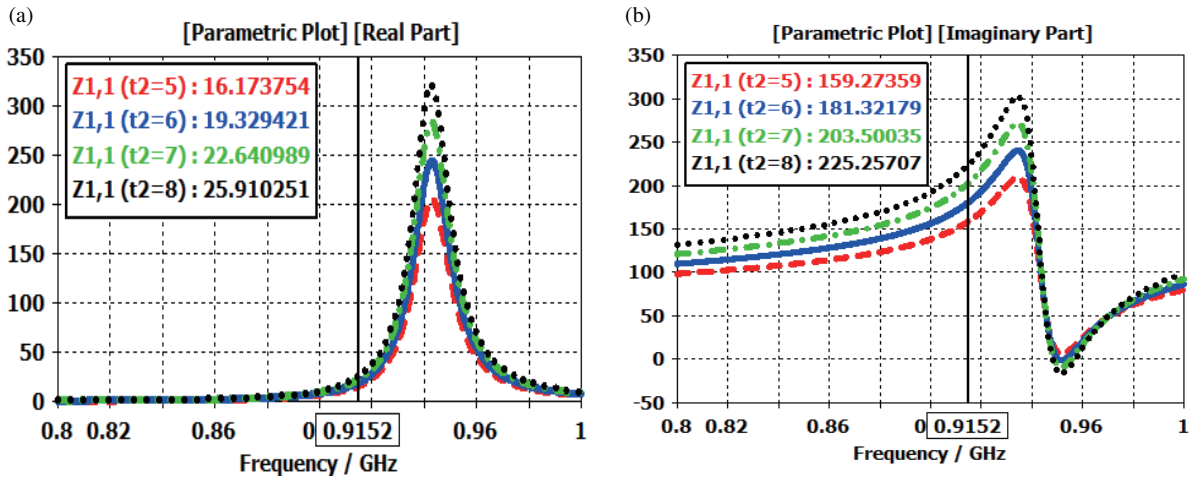

FIGURE 5. The suggested antenna's simulated input impedance for diverse values of $t2$, (a) real part and (b) imaginary part.

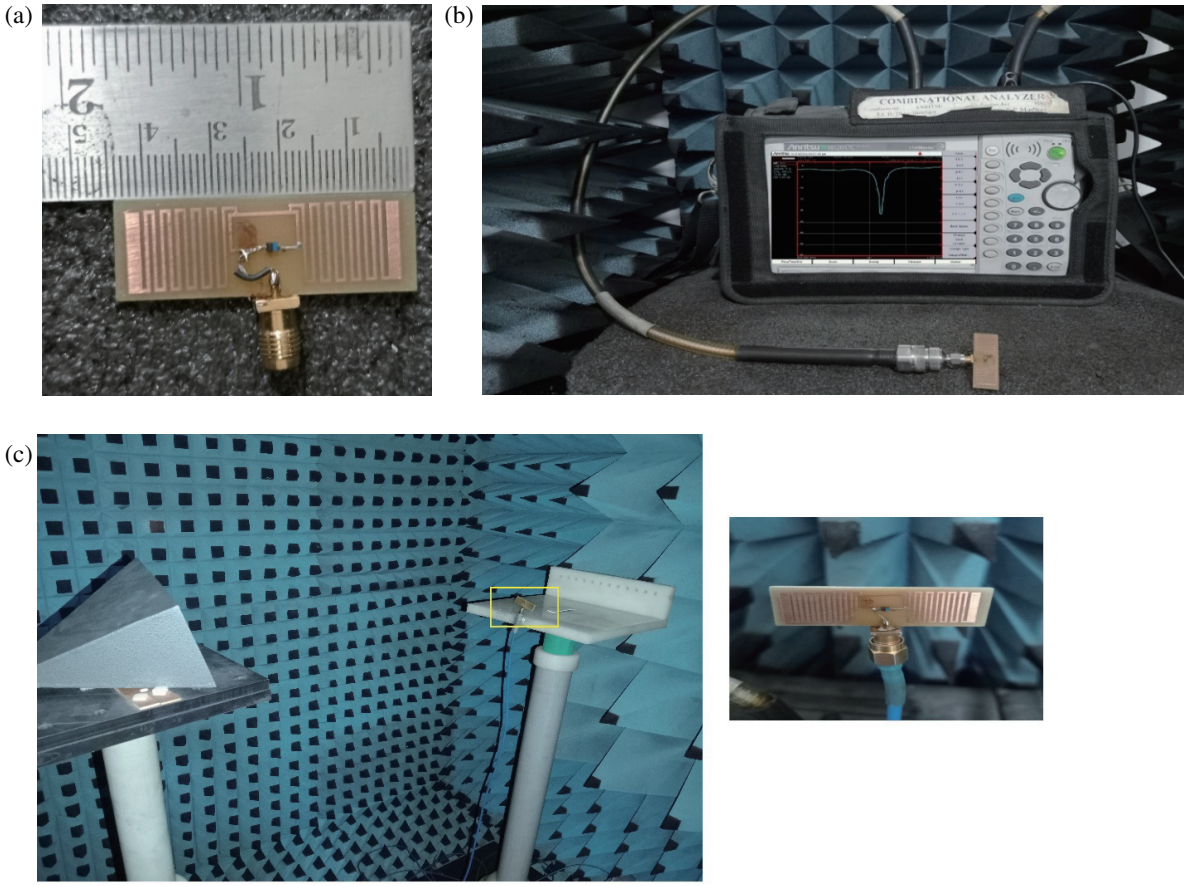

FIGURE 6. Proposed UHF RFID Tag antenna. (a) Fabricated prototype. (b) Measurement set up using VNA. (c) Radiation performance measurement set up in an anechoic chamber.

value between 11.65 mm and 12.4 mm with a stepping stone of 0.25 mm, the resonant frequency is slightly shifted to lower frequencies. In conclusion, it is possible to control the desired resonance frequency by modifying the radiator length (R2). As shown in Fig. 4, the resonance frequency of 915.2 MHz is reached when the value of R2 is set to 12.15 mm.

3.3. Impact of Varying the Height ``$t2$" of T-Matching Structure Rectangle on the Input Impedance

To study the impact of varying the height '$t2$' of the T-matching structure on the tag antenna's input impedance, '$t2$' was adjusted from 5 mm to 8 mm in 1 mm increments, while retaining the values of the other parameters unchanged, as illustrated in

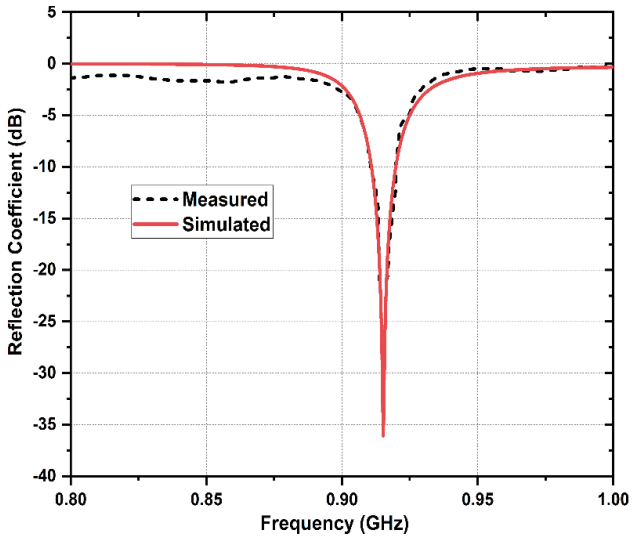

FIGURE 7. Simulated and measured reflection coefficients.

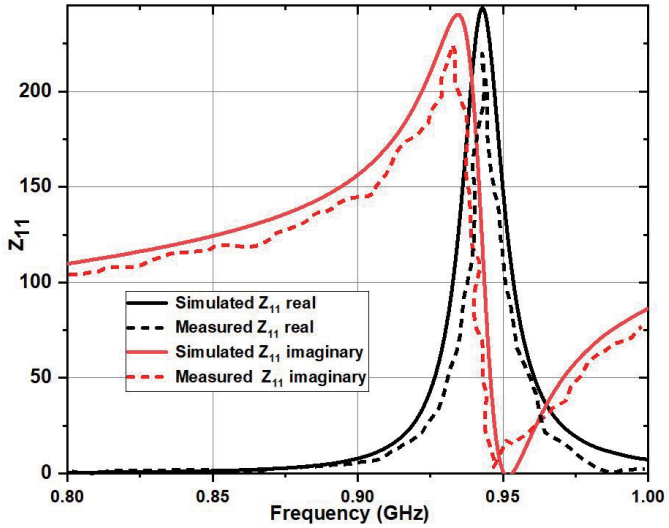

FIGURE 8. Simulated and measured input impedance.

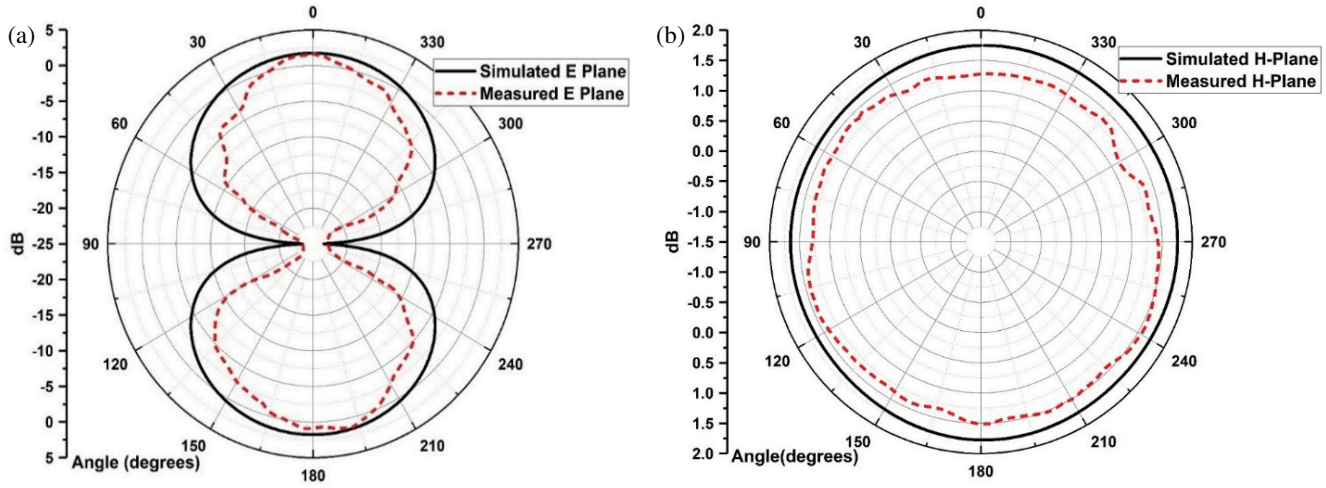

FIGURE 9. Simulated and measured radiation patterns of the proposed tag. (a) E-plane. (b) H-plane.

Fig. 5. The results indicate that the input resistance (real part) increased from 16.17 Ω to 25.91 Ω, and the reactance (imaginary part) increased from 159.27 Ω to 225.25 Ω as "$t2$" was increased at the resonant frequency of 915.2 MHz. Changing "$t2$" had a minor effect on resistance, but a significant effect on reactance. In addition, the best value of $t2 = 6$ mm ensures that the antenna and chip exhibit appropriate conjugate matching.

4. RESULTS AND DISCUSSION

In order to evaluate the simulation study, a model of the suggested ta's antenna was built and put through testing. This fabricated prototype appears in Fig. 6(a). Fig. 6(b) illustrates the proposed antenna's measuring setup utilizing a VNA. The radiation characteristics provided by this designed antenna are tested through the experimental setup placed in an anechoic chamber for accurate measurements. Inside this anechoic chamber, the horn antenna is used as a transmitter, and the suggested printed tag antenna is connected over the receiving side for measurement. The turn table mechanism is connected with software to analyze the radiation characteristics in E- and H-planes. The measured result for the reflection coefficient against frequency is compared with the simulated one as illustrated in Fig. 7. At 915.2 MHz, a simulated reflection coefficient of -36 dB is achieved, compared to a measured value of -24 dB. Based on the results, the simulated bandwidth of the proposed antenna is 9 MHz (910.8–919.8 MHz) whereas the corresponding measured bandwidth is 7.9 MHz ranging from 911.5 MHz to 919.4 MHz. These results indicate the correspondence between measured and simulated results within the resonant band. Fig. 8 displays both simulated and measured input impedance curves for the designed tag antenna. The measured antenna impedance is approximately $15 + j172.3\Omega$ compared to a simulated impedance of $19.32 + j181.3\Omega$ at the resonant frequency. The antenna's simulated and measured input impedance values are rather near

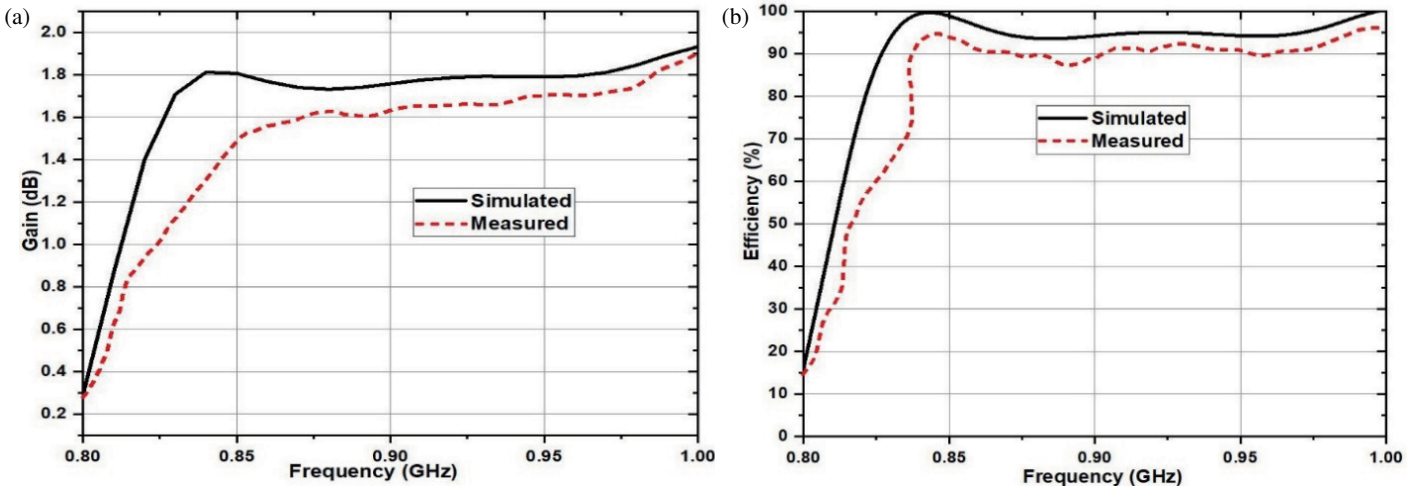

FIGURE 10. Simulated and measured, (a) gain, (b) tag radiation efficiency vs frequency.

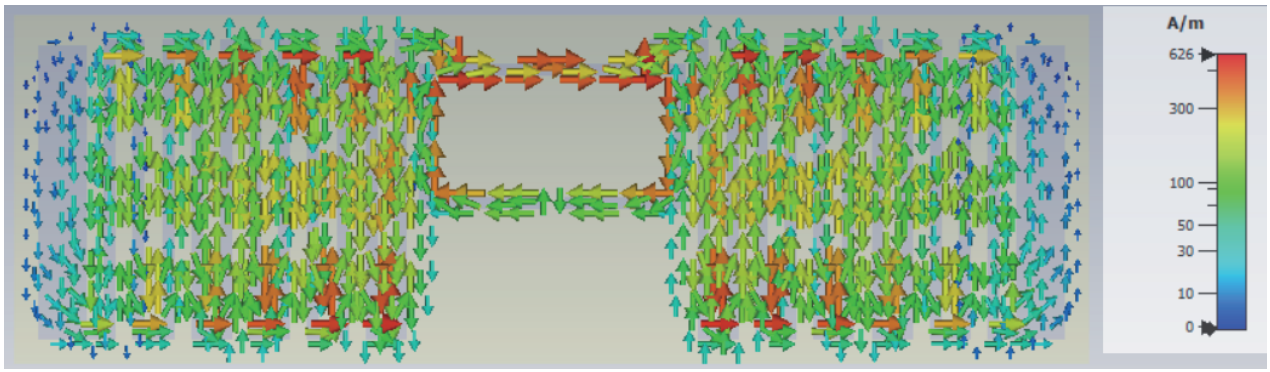

FIGURE 11. Surface current distribution of the proposed design at 915 MHz.

the chip's conjugate impedance of $18.43 - j181.2\Omega$, indicating that proper impedance matching is needed for maximum power transfer. Fig. 9 depicts both simulated and measured 2D radiation patterns, in the E and H planes. This antenna has bidirectional radiation in the E-plane (Fig. 10(a)) and omnidirectional one in the H-plane (Fig. 10(b)) for both simulated and measured results indicating the concordance between these data.

The performance of the suggested tag antenna was also assessed based on gain and radiation efficiency. Fig. 10 (a) depicts the simulated and measured gains of the designed tag antenna versus frequency. The measured gain has a peak value of approximately 1.65 dB, whereas the simulated value is 1.78 dB for the 915 MHz frequency. The measured maximum gain is 0.13 dB lower than the simulated result. Results in terms of measurement and simulatuib differ slightly, which could be caused by manufacturing and measuring tolerances. Although the antenna is miniatured in size, it represents an acceptable gain. In addition, Fig. 10(b) displays the tag's simulated and measured radiation efficiencies according to frequency. The proposed antenna has an efficiency over 90% throughout the operating band. It is around 95% for the simulated result and 90% for the measured one at 915 MHz resonance frequency.

Figure 11 illustrates the surface current distribution at 915 MHz to further analyze the tag antenna's radiation performance. The maximum magnitude of the surface current is observable across the loop of the T-match structure ("T-match structure rectangle"), which excites the meandering radiating element. As a result, exciting current distribution occurs along the entire length of the meandering antenna, demonstrating the important role played by the T-shaped matching structure in the tag's performance.

RFID system performance is also evaluated in terms of the reading range, a metric that denotes the maximum reading distance of the tag from the reader. It can be determined using the Friis formula [19], as shown below:

$$r = \frac{\lambda}{4\pi}\sqrt{\frac{\text{EIRP} \cdot \text{G}_{\text{tag}} \cdot \tau}{P_{th}}} \tag{2}$$

where λ signifies the free-space wavelength at the operating frequenc; EIRP is the effective isotropic radiated power (4 W in the USA) as defined according to local country regulations; P_{th} is the minimal power threshold required to activate the RFID chip, and its value has been specified for the Alien Higgs-4 chip as -20 dBm; G_{tag} is the gain of the designed tag antenn; τ is

TABLE 2. Performance comparison of the suggested tag antenna with that of other tag antennas in the literature.

Ref	Substrate thickness (mm)	Tag size (mm^2)	Tag volume (mm^3)	Dielectric materia	Frequency of oération (MHz)	Gain (dB/dBi)	Read range (m)
[21]	1.575	67×110	11607.75	Rogers RT/Duroid	915	1.2 dB	15.05
[22]	1.6	50×12	96	FR-4	915	−3.61 dB	4.06
[23]	0.8	58×46	2134.4	FR-4	915	2.19 dBi	18.37
[24]	0.5	48×13.7	328.8	Polyethylene (PET)	925	—	3.5
[25]	1.6	50×22	1760	FR-4	915	—	10.36
[26]	0.8	54×24	1036.8	FR-4	915	1.31 dB	16.13
[27]	1.6	50×22	1760	FR-4	867	1.2 dB	13.94
[28]	1.6	36×25	1440	FR-4	910	−0.135 dB	3
[29]	1.6	50×67	5360	FR-4	925	—-	4.4
[30]	1.6	120×67	12864	RT/duroid 5880	865	−0.47 dBi	13.9
[31]	3.18	40×40	5088	Polyethylene (PET)	916	−2.21 dB	9.5
This work	**0.8**	44.4×14.4	**511.488**	**Polytetrafluoroethylene (PTFE)**	**915.2**	**1.78 dB**	**18.41**

the coefficient of power transmission representing the antenna's impedance matching with the RFID chip, and it is given by [20]:

$$\tau = \frac{4 \cdot R_{chip} \cdot R_a}{|Z_a + Z_{chip}|^2}, \quad 0 \leq \tau \leq 1 \tag{3}$$

where $_{Za} = Ra + jXa$ represents the tag antenna's impedance, and $Z_{chip} = R_{chip} + j_{Xchip}$ denotes the IC chip impedance. The theoretical read range is found to be 18.4 m at 915 MHz.

5. COMPARATIVE ANALYSIS OF PERFORMANCE WITH STATE-OF-THE-ART

To highlight the potential of the suggested tag, a comparison of its performances with some recently developed tags has been carried out. Each of these antennas is designed to operate in a single frequency band. The comparison is illustrated in Table 2, taking into account size, gain, and reading range.

As seen from the Table, the prescribed tag has a smaller dimension in comparison with the tags in [21–23, 25–31], indicating its compactness. Nevertheless, the volume of our proposed antenna is greater than that of the antenna in [24], as the latter is thinner than our antenna. Besides offering compactness, it offers higher gain than the other tags except for the one in [23]. However, the last has a larger size than our suggested antenna design. Furthermore, our antenna has a better reading range concerning tags in [21, 22, 24–31] and is almost identical to that of [23]. Hence, owing to its compact size, long reading range, and high gain, the designed tag performs competitively and is appropriate for UHF-RFID applications.

6. CONCLUSION

In this research, a new UHF RFID tag antenna, operating at 915 MHz is designated and studied. It has a miniatured size of $44.4 \times 14.4 \times 0.8\,mm^3$. The proposed tag antenna structure has been configured through the use of a meandering line technique. Proper conjugate matching of the antenna and the Alien Higgs-4 IC is obtained by using a T-match feed network. The optimum tag has a read range of 18.41 m with a gain of 1.78 dB and a radiation efficiency of 96%. The antenna's simulated performance is validated by testing the fabricated prototype through an experimental setup. Simulated and measured results match closely. The above characteristics make the antenna suitable for mass production, serving as an RFID tag antenna at the UHF band.

REFERENCES

[1] Vijayalakshmi, J., V. Dinesh, P. A. Sivsankgari, S. Saranya, and V. Sanju, "A ultra high frequency (UHF) RFID antenna design for food quality and safety," *Int. J. Recent Technol. Eng.*, Vol. 8, No. 6, 1013–1022, 2020.

[2] Singh, A. K. and A. K. Singh, "A meandered inductive loop based RFID tag antenna for luggage tracking," *Progress In Electromagnetics Research C*, Vol. 132, 103–115, 2023.

[3] Ali, W., N. Nizam-Uddin, W. M. Abdulkawi, A. Masood, A. Hassan, J. A. Nasir, and M. A. Khan, "Design and analysis of a quad-band antenna for iot and wearable RFID applications," *Electronics*, Vol. 13, No. 4, 700, 2024.

[4] Wang, L., Z. Luo, R. Guo, and Y. Li, "A review of tags anti-collision identification methods used in RFID technology," *Electronics*, Vol. 12, No. 17, 3644, 2023.

[5] Abdulghafor, R., S. Turaev, H. Almohamedh, R. Alabdan, B. Almutairi, A. Almutairi, and S. Almotairi, "Recent advances in passive UHF-RFID tag antenna design for improved read range in product packaging applications: A comprehensive review," *IEEE Access*, Vol. 9, 63 611–63 635, 2021.

[6] Jouali, R., H. Ouahmane, J. Khan, M. Liaqat, A. Bhaij, S. Ahmad, A. Haddad, and M. Aoutoul, "Improved stable read range of the RFID tag using slot apertures and capacitive gaps for outdoor localization applications," *Micromachines*, Vol. 14, No. 7, 1364, 2023.

[7] Alibakhshikenari, M., B. S. Virdee, A. A. Althuwayb, K.-D. Xu, C. H. See, S. Khan, I. Park, F. Falcone, and E. Limiti, "Novel concentric hexagonal-shaped RFID tag antenna with T-shaped stub matching," *IEEE Journal of Radio Frequency Identification*, Vol. 6, 112–120, 2021.

[8] Sharif, A., R. Kumar, K. Arshad, K. Assaleh, H. T. Chattha, M. A. Imran, and Q. H. Abbasi, "Nature-inspired spider web shaped UHF RFID reader antenna for IOT and healthcare applications," *Scientific Reports*, Vol. 13, No. 1, 14017, 2023.

[9] Hamani, A., M. C. E. Yagoub, T.-P. Vuong, and R. Touhami, "A novel broadband antenna design for UHF RFID tags on metallic surface environments," *IEEE Antennas and Wireless Propagation Letters*, Vol. 16, 91–94, 2016.

[10] Choudhary, A., D. Sood, and C. C. Tripathi, "Wideband long range, radiation efficient compact UHF RFID tag," *IEEE Antennas and Wireless Propagation Letters*, Vol. 17, No. 10, 1755–1759, 2018.

[11] Babar, A. A., T. Bjorninen, V. A. Bhagavati, L. Sydanheimo, P. Kallio, and L. Ukkonen, "Small and flexible metal mountable passive UHF RFID tag on high-dielectric polymer-ceramic composite substrate," *IEEE Antennas and Wireless Propagation Letters*, Vol. 11, 1319–1322, 2012.

[12] Jaakkola, K., "Small on-metal UHF RFID transponder with long read range," *IEEE Transactions on Antennas and Propagation*, Vol. 64, No. 11, 4859–4867, 2016.

[13] Li, H., J. Zhu, and Y. Yu, "Compact single-layer RFID tag antenna tolerant to background materials," *IEEE Access*, Vol. 5, 21 070–21 079, 2017.

[14] Oliveira, D. B. and E. J. Silva, "Design of the compact UHF RFID meander-line antenna loaded with CPW elements," *Aeu-international Journal of Electronics and Communications*, Vol. 77, 57–60, 2017.

[15] Zamora, G., S. Zuffanelli, F. Paredes, F. Marti, J. Bonache, *et al.*, "Design and synthesis methodology for UHF-RFID tags based on the T-match network," *IEEE Transactions on Microwave Theory and Techniques*, Vol. 61, No. 12, 4090–4098, 2013.

[16] Liu, Q., Y. Yu, and S. He, "Capacitively loaded, inductively coupled fed loop antenna with an omnidirectional radiation pattern for UHF RFID tags," *IEEE Antennas and Wireless Propagation Letters*, Vol. 12, 1161–1164, 2013.

[17] Sharif, A., J. Ouyang, Y. Yan, A. Raza, M. A. Imran, and Q. H. Abbasi, "Low-cost inkjet-printed RFID tag antenna design for remote healthcare applications," *IEEE Journal of Electromagnetics, RF and Microwaves in Medicine and Biology*, Vol. 3, No. 4, 261–268, 2019.

[18] Higgs 4 RFID IC, "Alien technology," Accessed: Oct. 8, 2020. [Online]. Available: https://www.alientechnology.com/products/ic/higgs-4/.

[19] Marrocco, G., "The art of UHF RFID antenna design: impedance-matching and size-reduction techniques," *IEEE Antennas and Propagation Magazine*, Vol. 50, No. 1, 66–79, 2008.

[20] Barman, B., S. Bhaskar, and A. K. Singh, "Spiral resonator loaded S-shaped folded dipole dual band UHF RFID tag antenna," *Microwave and Optical Technology Letters*, Vol. 61, No. 3, 720–726, 2019.

[21] Raihani, H., A. Benbassou, M. E. Ghzaoui, J. Belkadid, and S. Das, "Patch antennas with T-match, inductively coupled loop and nested-slots layouts for passive UHF-RFID tags," *Journal of Nano-and Electronic Physics*, Vol. 13, No. 3, 03033, 2021.

[22] Bhaskar, S. and A. K. Singh, "A compact meander line UHF RFID antenna for passive tag applications," *Progress In Electromagnetics Research M*, Vol. 99, 57–67, 2021.

[23] Bansal, A., S. Sharma, and R. Khanna, "Linearly tapered meander line broadband monopole tag antenna with T-match for ultra high frequency radio frequency identification applications," *International Journal of RF and Microwave Computer-aided Engineering*, Vol. 30, No. 11, e22423, 2020.

[24] Xuan, X., L. Lv, and K. Li, "A miniaturized meandered dipole UHF RFID tag antenna for flexible application," *International Journal of Antennas and Propagation*, Vol. 2016, No. 1, 2951659, 2016.

[25] Bhaskar, S. and A. K. Singh, "Capacitive tip loaded linearly tapered meander line antenna for UHF RFID tag applications," in *2017 IEEE Applied Electromagnetics Conference (AEMC)*, 1–2, Aurangabad, India, 2017.

[26] El Hachimi, Y. and A. Farchi, "A novel compact antenna for passive UHF RFID tag using π-match and meander techniques," in *3rd International Conference on Computing and Wireless Communication Systems*, 2019.

[27] Gmih, Y. and A. Farchi, "A new design of a miniaturized UHF-RFID passive tag antenna based on L-shape radiators with meandered dipole," in *3rd International Conference on Computing and Wireless Communication Systems*, 103, 2019.

[28] Fazilah, A. F. M., M. Jusoh, A. Zakaria, T. Sabapathy, M. F. Ibrahim, M. N. Osman, M. N. Yaasin, S. Malhotra, and H. A. Rahim, "Design of compact UHF-RFID tag antenna with meander line technique," in *Iop Conference Series: Materials Science and Engineering*, Vol. 767, No. 1, 012058, 2020.

[29] Kamalvand, P., G. K. Pandey, and M. K. Meshram, "A single-sided meandered-dual-antenna structure for UHF RFID tags," *International Journal of Microwave and Wireless Technologies*, Vol. 9, No. 7, 1419–1426, 2017.

[30] Singh, A. K. and S. Bhaskar, "A nested slot and T-match network based hybrid antenna for UHF RFID tag applications," *Progress In Electromagnetics Research C*, Vol. 125, 93–104, 2022.

[31] Lee, Y.-H., E.-H. Lim, F.-L. Bong, and B.-K. Chung, "Bowtie-shaped folded patch antenna with split ring resonators for UHF RFID tag design," *IEEE Transactions on Antennas and Propagation*, Vol. 67, No. 6, 4212–4217, 2019.